Double and Single ITCZs with and without Clouds

MAX POPP AND LEVI G. SILVERS

Program in Atmospheric and Oceanic Sciences, Princeton University, Princeton, New Jersey

ABSTRACT

A major bias in tropical precipitation over the Pacific in climate simulations stems from the models' tendency to produce two strong distinct intertropical convergence zones (ITCZs) too often. Several mechanisms have been proposed that may contribute to the emergence of two ITCZs, but current theories cannot fully explain the bias. This problem is tackled by investigating how the interaction between atmospheric cloud-radiative effects (ACREs) and the large-scale circulation influences the ITCZ position in an atmospheric general circulation model. Simulations are performed in an idealized aquaplanet setup and the longwave and shortwave ACREs are turned off individually or jointly. The low-level moist static energy (MSE) is shown to be a good predictor of the ITCZ position. Therefore, a mechanism is proposed that explains the changes in MSE and thus ITCZ position due to ACREs consistently across simulations. The mechanism implies that the ITCZ moves equatorward if the Hadley circulation strengthens because of the increased upgradient advection of low-level MSE off the equator. The longwave ACRE increases the meridional heating gradient in the tropics and as a response the Hadley circulation strengthens and the ITCZ moves equatorward. The shortwave ACRE has the opposite effect. The total ACRE pulls the ITCZ equatorward. This mechanism is discussed in other frameworks involving convective available potential energy, gross moist stability, and the energy flux equator. It is thus shown that the response of the large-scale circulation to the shortwave and longwave ACREs is a fundamental driver of changes in the ITCZ position.

1. Introduction

Most of the precipitation in Earth's tropics falls in a region of relatively small meridional extent that migrates with the seasons. Dynamically, this region of strong precipitation is characterized by strong mean upward motion and low-level convergence of winds and hence this region is commonly referred to as an intertropical convergence zone (ITCZ). Simulating and understanding the mechanisms governing the meridional extent, the amount of precipitation, and the position of the ITCZ is thus a necessary component of predicting how variations and long-term trends in the climate may affect tropical precipitation. However, the full extent of mechanisms that affect the properties of the ITCZ is not yet well understood (Faulk et al. 2017) and state-of-the-art climate models struggle to represent several aspects of the ITCZ accurately (e.g., Lin 2007; Bollasina and Ming 2013; Hwang and Frierson 2013; Li and Xie 2014; Siongco et al. 2015).

A pressing problem in climate simulations when compared to observations is the too frequent and too pronounced occurrence of two ITCZs in the eastern and western Pacific and over the Indian Ocean in boreal summer (Lin 2007; Li and Xie 2014; Oueslati and Bellon 2015; Zhang et al. 2015), which may contribute to the spread of model climate sensitivity (Tian 2015). Even in the zonal and annual mean the two ITCZs in models tend to be too far from the equator when compared to observations (Lin 2007; Li and Xie 2014; Adam et al. 2016). We will refer here to this "double-ITCZ problem" in terms of the temporal- and zonal-mean distance of the ITCZs from the equator (note that other definitions exist of the double-ITCZ bias or problem). The problem is most prominent in coupled simulations but it is also apparent in simulations with prescribed sea surface temperatures (SSTs) even on hemispherically symmetric aquaplanets (completely water-covered planets; e.g., Numaguti 1993; Williamson 2012; Möbis and Stevens 2012; Landu et al. 2014; Harrop and Hartmann 2016; Fläschner 2016).

ⓐ Denotes content that is immediately available upon publication as open access.

Corresponding author: Max Popp, mpopp@princeton.edu

The absence of hemispherical asymmetries in aquaplanet simulations has made it a popular test bed to identify and understand mechanisms contributing to the double-ITCZ problem.

So far, several factors have been identified that may contribute to the double-ITCZ problem, such as weak meridional surface-temperature gradients in the tropics (Dahms et al. 2011; Oueslati and Bellon 2013b), a low entrainment rate in the convective parameterization (Möbis and Stevens 2012; Oueslati and Bellon 2013a), the resolution of the model (Landu et al. 2014), and, most recently, weak atmospheric cloud-radiative effects (ACREs) (Harrop and Hartmann 2016; Fläschner 2016). However, the influence of ACREs on the tropical large-scale dynamics (Voigt et al. 2014a), and in particular how ACREs contribute to the double-ITCZ problem, is not well understood. Harrop and Hartmann (2016) and Fläschner (2016) show that the total ACRE pulls the ITCZ toward the equator, but it remains unclear how shortwave and longwave ACREs affect the ITCZ position individually, and a mechanism that explains the shift in ITCZ induced by the ACRE consistently across models is still missing. Therefore, this paper will investigate how the longwave and the shortwave ACREs interact with the tropical large-scale dynamics and thereby influence the ITCZ position in aquaplanet simulations. We will propose a mechanism that explains the shift in ITCZ using a framework that yields consistent results across models. We will for the first time apply and compare several diagnostic and prognostic frameworks for the ITCZ position to this problem. These frameworks are based on low-level moist static energy (MSE), gross moist stability, and the energy-flux equator.

ACREs have been shown to affect many aspects of the tropical large-scale circulation in GCMs, such as the strength of the large-scale circulation (Randall et al. 1989; Harrop and Hartmann 2016), vertical velocity (Slingo and Slingo 1988; Randall et al. 1989; Harrop and Hartmann 2016), the low-level convergence (Randall et al. 1989; Harrop and Hartmann 2016), the strength of the Walker circulation (Sherwood et al. 1994), the magnitude of El Niño–Southern Oscillation (Rädel et al. 2016), and the Madden–Julian oscillation (Crueger and Stevens 2015). Other studies suggest that ACREs influence the ITCZ position (Kang et al. 2008; Zhang et al. 2010; Hwang and Frierson 2013; Voigt et al. 2014a,b; Harrop and Hartmann 2016; Fläschner 2016) and Harrop and Hartmann (2016) recently investigated the influence of ACREs on the ITCZ systematically by using the output of six models taking part in the Clouds On–Off Klimate Intercomparison Experiment (COOKIE; see Stevens et al. 2012). We choose a different approach to

study the influence of ACRE on the position of the ITCZ. We perform a multitude of simulations with a single state-of-the-art atmospheric GCM. This allows us to tailor the experimental setup and model output to our needs. Thus we investigate for the first time how the longwave and the shortwave ACREs affect the ITCZ position separately. This is important for attributing model biases in ITCZ position to biases in ACREs, since the contribution of the longwave and shortwave ACRE biases to the total ACRE bias could differ between models. Furthermore, we modify the model to obtain specialized output for the task at hand. This allows us to put forward an alternative mechanism by which ACREs individually affect clouds.

In brief, our mechanism is as follows: ACREs enhance the atmospheric energy uptake in the deep tropics and the Hadley circulation responds to this by strengthening in order to export more energy away from the tropics. This circulation strengthening shifts the low-level MSE peak (and hence the ITCZ latitude) equatorward due to the negative MSE flux by the lower branch of the Hadley cell. Oueslati and Bellon (2013b) also found that changes in low-level winds are important for the ITCZ position when studying the effect of surface-temperature forcings, but this is the first study to implement the mechanism into a MSE framework and to find the mechanism for fixed surface temperatures. In contrast to the mechanism based on convective available potential energy (CAPE) suggested by Harrop and Hartmann (2016), our mechanism based on the width of the low-level MSE peak as a predictor of the ITCZ position gives consistent results across all models. A framework based on gross moist stability gives an equally good prediction of the ITCZ position, whereas estimating the ITCZ position from the zero of the mean meridional energy transport only yields mixed results.

This paper is organized as follows: In sections 2a and 2b we introduce the employed GCM and the applied boundary conditions. The experimental setup is outlined in sections 2c and 2d. We will first show how the ACREs affect the large-scale circulation in steady state (section 3a and 3b) and identify the mechanism at work. We will then investigate how changes in the distribution of low-level MSE affect the ITCZ position and we will make use of transient simulations for that purpose (sections 4a and 4b). We will also discuss in this context how the suggested mechanism relates to the width of the ITCZ (section 4c) and to the strength of the Hadley circulation (section 4d). Subsequently we will discuss the shifts of ITCZ in the framework of zonal-mean convective CAPE (section 5a), gross moist stability (section 5b), and the zero-crossing of the mean meridional energy

transport (section 5c). We end the paper with a discussion of the implications of this study and with the main conclusions (section 6).

2. Methods

a. Model

Simulations are performed with a developmental version of the latest GFDL atmospheric GCM (C96L32_am4g6) referred to here as $AM4_d$. The model uses a domain with approximately 100-km horizontal grid spacing and 32 vertical levels extending from the surface to 10 Pa. The dynamical core uses a cubed sphere with each face having 96×96 grid points. For the simulations presented in this study, the prognostic aerosol was turned off to allow for a simple aquaplanet experiment (APE) configuration [see Neale and Hoskins (2000) and Williamson (2012)]. Instead the cloud condensation nuclei concentration number was prescribed as $10^8 m^{-3}$. With the exception of the convective cloud parameterizations, the physics of $AM4_d$ is quite similar to that of AM3 (Donner et al. 2011). The convective parameterization of $AM4_d$ is a bulk two-plume mass flux scheme and is a modification of the shallow convective parameterization described in Bretherton et al. (2004). For details of the model physics see Zhao et al. (2016) and Donner et al. (2011). For the full documentation and climatology of the documented version of AM4 please refer to Zhao et al. (2017, manuscript submitted to *J. Adv. Model. Earth Syst.*).

To turn off a particular component of the ACREs we set the fractional cloud cover that is used for radiative computations of that component to zero at all levels. This option has been applied to both the shortwave and longwave components of the radiative transfer calculations. Turning the ACREs off only affects the radiation; the cloud condensate is still perceived by the model's moist thermodynamics and dynamics. In that sense, this option can be thought of as making the clouds transparent to radiation in the longwave, in the shortwave, or in both parts of the spectrum.

b. Boundary conditions

We use $AM4_d$ in aquaplanet mode to utilize the interhemispheric symmetry and the shorter spinup times. Orbital parameters are set to perpetual-equinox conditions with general Earth-like settings for the rotation velocity, mass, and global- and temporal-mean insolation. The ozone concentration is zonally uniform but varies in the meridional and vertical direction according to the APE protocol (Neale and Hoskins 2000; Williamson 2012). Atmospheric concentrations of other

greenhouse gases (except water vapor) are assumed to be uniformly mixed following the APE protocol (1650 ppbv for CH_4, 306 ppbv for N_2O, and 348 ppmv CO_2). The lower boundary is set to a fixed SST pattern that varies in the meridional direction but is constant in time and zonal direction. This SST pattern was modeled with a simple mathematical function to represent the observed zonal-mean SST distributions and is referred to as QOBS following Neale and Hoskins (2000).

c. Experiments

1) STEADY-STATE EXPERIMENTS

The four steady-state APE simulations presented here run for 11 years. The first six years of data are discarded to eliminate spinup noise and only the last 5 years in steady state are considered. The four experiments are both longwave and shortwave ACREs turned off (ACREoff), longwave ACRE turned on and shortwaveACREturned off (ACREonLW), longwaveACREturned off and shortwaveACREturned on (ACREonSW), and both shortwave and longwave ACRE turned on (ACREon).

2) TRANSIENT SIMULATIONS

In addition to steady-state experiments, we perform two ensembles of transient simulations with 10 members each to better understand the mechanisms behind the changes in ITCZ position. Both ensembles start from the steady-state conditions of the ACREoff experiment and run for one year. In the first ensemble the longwave ACRE is turned on at the beginning of the simulations and in the second ensemble the shortwave ACRE is turned on at the beginning of the simulations.

d. Further considerations

Traditional simulations of the atmosphere (e.g., AMIP and weather prediction) correspond to our ACREon experiment. When comparing experiments with and without ACREs, the ACREon experiment has often been used as the reference state. In contrast, this study uses the ACREoff experiment as the reference because we have found it more natural to investigate the response of the climate to ACREs being turned on. Previous studies (Slingo and Slingo 1988; Randall et al. 1989; Crueger and Stevens 2015; Harrop and Hartmann 2016) of ACREs have focused on comparisons between the ACREoff and ACREon experiments. However, the strong response of land surfaces to changes of shortwave radiation makes an interpretation of the ACREoff experiment solely in terms of cloud changes difficult. Therefore, the next round of the Cloud-Forcing Model Intercomparison Project phase 3 (CFMIP3) recommends
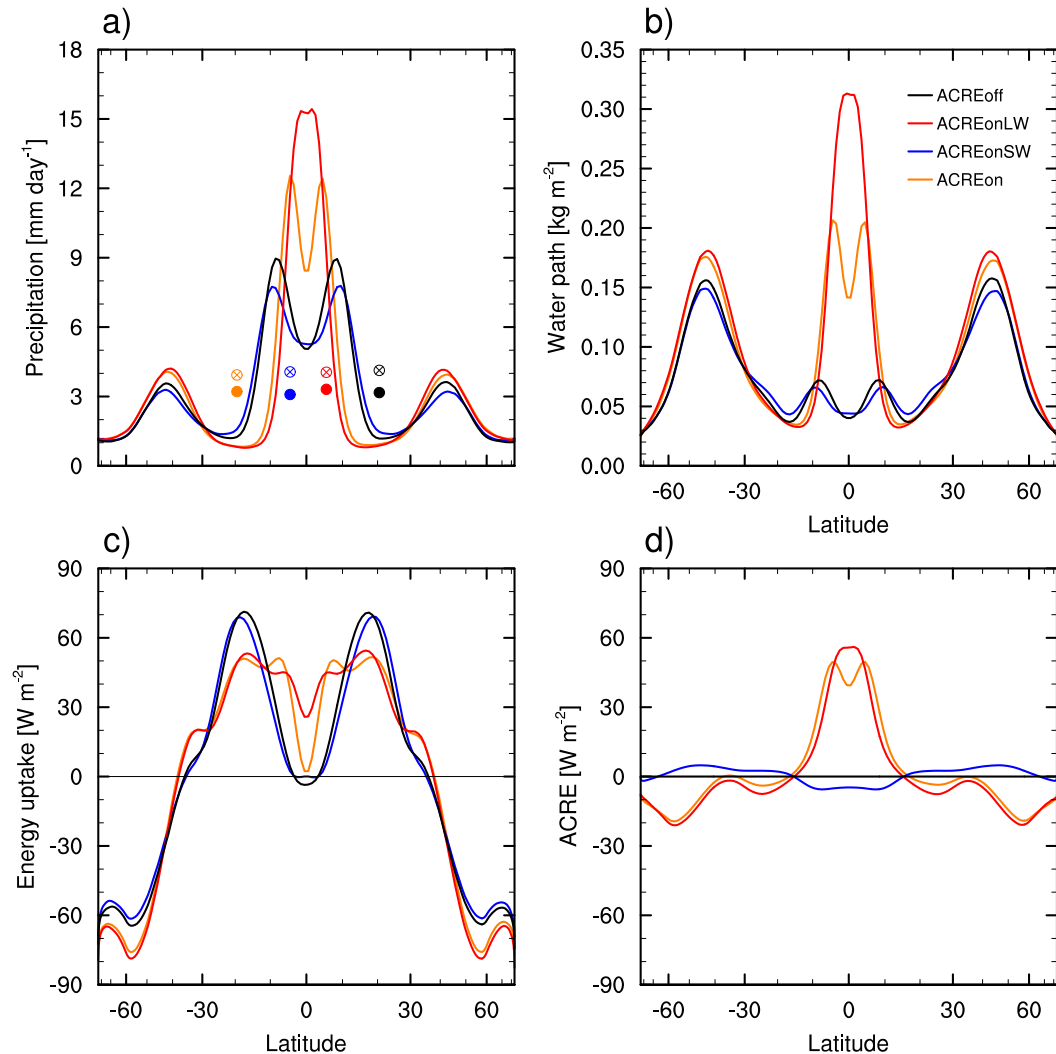
FIG. 1. Zonal-mean quantities in steady state: (a) the total (convective + large-scale) precipitation, (b) the vertically integrated total (liquid + frozen) water path, (c) the atmospheric energy uptake, and (d) the ACRE. Colors represent the individual experiments ACREoff (black), ACREonLW (red), ACREonSW (blue), and ACREon (orange). The filled circles show the global and the crossed circles the tropical means (from 30°S to 30°N) of precipitation in (a). The horizontal location of the dots is only for visual separation and does not have any particular meaning. Note that the horizontal axes are scaled with the cosine of the latitude.

ACREonLW experiments to isolate the cloud response (Webb et al. 2017). This concern is irrelevant in our APEs because of the fixed lower boundary. As is shown in the following section, each of the four experiments investigated here reveals interesting interactions between clouds and radiation. The results obtained with our approach do not include the response of the surface temperature to changes in ACREs. However, fixing the surface temperature has the advantage of taking out a feedback and thus facilitates the interpretation of the atmospheric response to changes in ACREs, which by itself is not yet well understood. Furthermore, the fixed surface temperature experiments follow a well-defined protocol

(APE) that allows us to easily compare our results to previous ones.

3. The effect of shortwave and longwave ACREs on the position of the ITCZ

a. Shifts in the ITCZ and changes in the large-scale circulation

In both the ACREoff and the ACREon simulations there are two ITCZs (Fig. 1a). We identify the ITCZ here as the hemispheric maximum in zonal-mean precipitation. The ITCZs are, however, considerably farther away
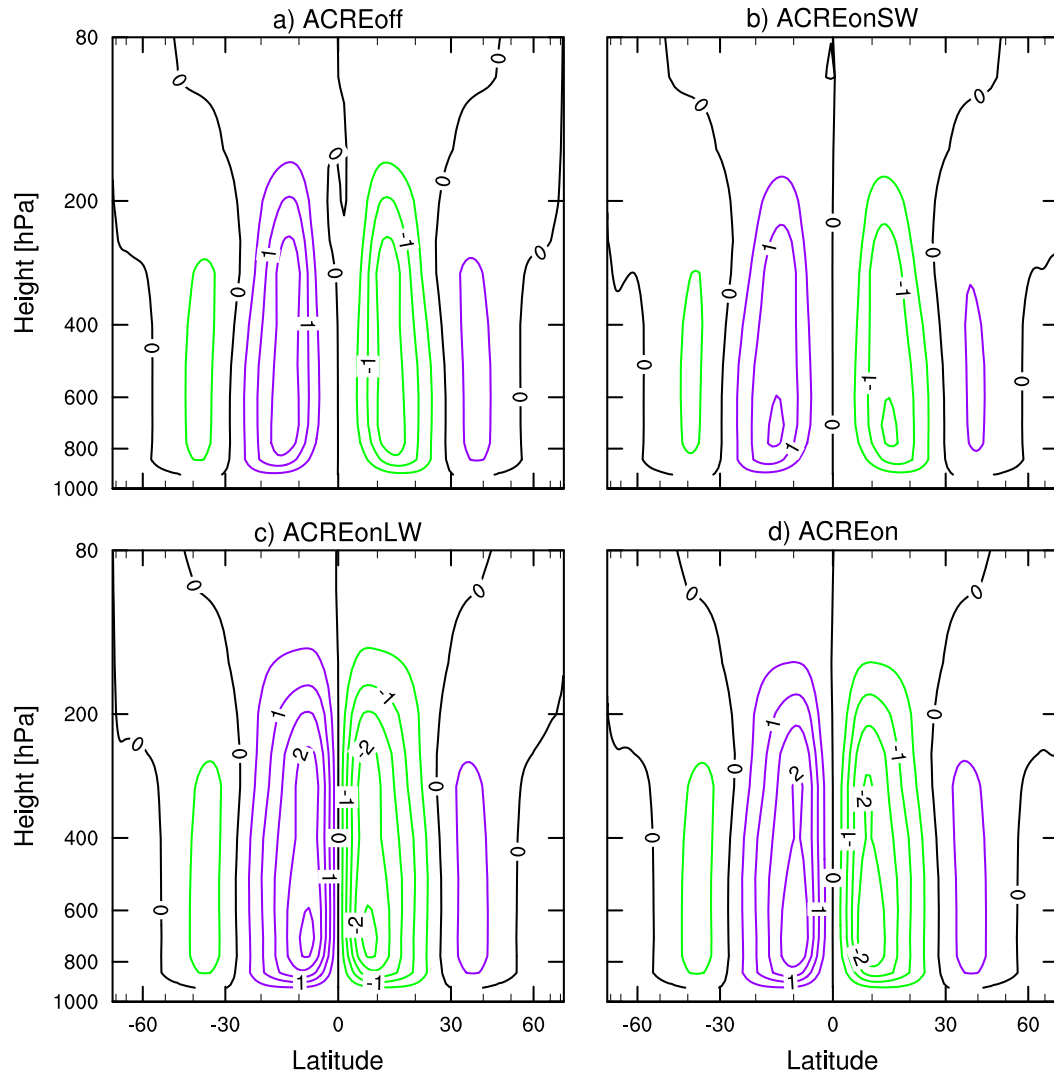
FIG. 2. Zonal-mean mass streamfunction in steady state for (a) ACREoff, (b) ACREonSW, (c) ACREonLW, and (d) ACREon. Green contours denote clockwise and violet contours counterclockwise rotation. The zero value is denoted by black contours. The depicted contours increase in steps of $0.5 \times 10^{11}\,\mathrm{kg\,s^{-1}}$. Note that the horizontal axes are scaled with the cosine of the latitude and that the vertical coordinates are logarithmic.

from the equator in the ACREoff experiments than in the ACREon experiments. Hence, the net ACRE pulls the ITCZs toward the equator (Fig. 1a). If we turn only the longwave ACRE on, the ITCZs move all the way to the equator to form a single ITCZ. If, by contrast, only the shortwave ACRE is turned on, then the ITCZ moves farther away from the equator (Fig. 1a). So the longwave and the shortwave ACRE have opposite effects on the position of the ITCZ. The peak of the precipitation at the ITCZ increases in magnitude with decreasing latitude of the ITCZ position. The difference between experiments does not, however, exceed $0.23\,\mathrm{mm\,day^{-1}}$ in the global mean and $0.20\,\mathrm{mm\,day^{-1}}$ in the tropical mean (defined here from 30°S to 30°N) because the increase in

precipitation at the ITCZ with decreasing latitude of the ITCZ is offset by a decrease in precipitation in the subtropical subsidence regions (Fig. 1a). So the closer the ITCZ moves to the equator, the less precipitation falls off the equator. This is consistent with an increase in the strength of the Hadley circulation with decreasing latitude of the ITCZ (Fig. 2): Stronger mean upward vertical velocities in the ITCZ promote an increase in zonal-mean precipitation in the upwelling region and stronger mean downward vertical velocities suppress precipitation in the subsidence region.

The increase in the strength of the Hadley circulation with decreasing latitude of the ITCZ is consistent with an increase in zonal-mean atmosphere energy uptake

(Fig. 1c) at the equator. The atmospheric energy uptake is defined as the net downward (=downward − upward) top-of-the-atmosphere energy flux minus the net downward surface energy flux, and corresponds to the total net energy flux into the atmosphere. Since the global and temporal mean of the atmospheric energy uptake has to be zero, the energy uptake at higher latitudes has to decrease. Therefore, the atmosphere must export more energy from the equator to higher latitudes. In experiments with prescribed sea surface temperature the energy density that is transported can only change to a limited extent. The energy transport corresponds to the transported mass multiplied with the energy density [see Eq. (8)]. Hence, a substantial increase in poleward energy transport requires an increase in the strength of the large-scale circulation, if the energy density (and the depth of the circulation) does not change substantially.

The longwave ACRE increases the meridional gradient in atmospheric energy uptake because in the deep tropics convective clouds heat the atmosphere throughout their depth, whereas the longwave ACRE at higher latitudes predominantly warms the levels below the boundary layer clouds, but cools the atmospheric column as a whole (Figs. 1d and 3). Thus the longwave ACRE acts to strengthen the large-scale circulation. By contrast, the shortwave ACRE cools the atmosphere more in the tropics than at higher latitudes and therefore tends to weaken the large-scale circulation (Figs. 1d and 3).

Our results agree well with those from other models with ACREon and ACREoff experiments (Randall et al. 1989; Harrop and Hartmann 2016; Fläschner 2016). The ITCZ moves equatorward if the ACRE is turned on and the tropical large-scale circulation strengthens as well in all the models analyzed by Harrop and Hartmann (2016) and Fläschner (2016). We also find a strong increase in total (liquid + frozen) water path when ACREs are turned on, which suggests that the precipitation efficiency decreases in our model in this case (Fig. 1b). The increase in total water path is also consistent with stronger detrainment by the convection scheme when the longwave ACRE is turned on. Since the detrainment rate depends on the formulation of the convection scheme, this result could be strongly model dependent. However, the results of previous studies suggest an increase in convective detrainment by all models when the longwave ACRE is turned on, as evidenced by the increase in total water path (Harrop and Hartmann 2016). We find a slight decrease in tropical precipitation when the ACREs are turned on, but the decrease is not substantial (from 4.13 to 3.93 mm day^{-1}). This decrease occurs because the radiative cooling rate decreases when the ACREs are turned on (Fig. 3i). However, the clouds decrease the atmospheric cooling and thus

cause a warming of the deep tropical troposphere that is then communicated effectively meridionally over the entire tropics (Fig. 4c) due to the weak Coriolis force. As a consequence, the clear-sky cooling rate increases in most of the tropical troposphere and balances most of the cloud-radiative heating by clouds. The warming of the deep tropical troposphere is mostly due to the longwave ACRE (Fig. 4b). The shortwave ACRE tends to warm only the tropopause region (Fig. 4a).

b. The low-level MSE distribution as a predictor of the ITCZ position

To understand better how ACREs influence the position of the ITCZ, we will first choose an adequate predictor for the position of the ITCZ. Several predictors for the position of the ITCZ have been used that are based on gross-moist-stability arguments (e.g., Neelin and Held 1987; Kang et al. 2009) and arguments based on the zero crossing of the meridional energy transport by the atmosphere (e.g., Bischoff and Schneider 2014, 2016) and the meridional distribution of either low-level moist entropy or low-level MSE (e.g., Lindzen and Hou 1988; Emanuel et al. 1994; Privé and Plumb 2007). We start our discussion with the meridional distribution of low-level MSE, but will also discuss the other predictors in later subsections. The frozen MSE h has the units of an energy density and can be written as

$$h = c_p T + gz + Lq − L_f q_i, \tag{1}$$

where c_p is the specific heat capacity of air at constant pressure, T is the temperature, g is Earth's gravity acceleration, z is the height above sea level, L is the latent energy of vaporization, L_f is the latent heat of fusion, q is the specific humidity, and q_i is the specific mass of ice. Unlike the MSE, the frozen MSE is also conserved when freezing, melting, or sublimation occurs [the difference between the MSE and the frozen MSE is the last term in Eq. (1)]. However, the last term in Eq. (1) is usually small and therefore the frozen MSE is typically close to the MSE. All subsequent analysis uses the frozen MSE, but the lessons learned from this analysis would also apply to the MSE. Therefore, and for the sake of simplicity, we will subsequently drop the qualifier "frozen" and only talk of MSE. The MSE is approximately conserved in moist adiabatic ascent. Therefore, convection tends to be collocated with regions of small vertical gradients of MSE. Since the horizontal-mean gradients in MSE in the upper troposphere are small in the tropics (Sobel and Bretherton 2000), the atmosphere should be most unstable to convection in the region where the low-level MSE is largest. The MSE is a direct model output in our model. We find that the maximum of low-level
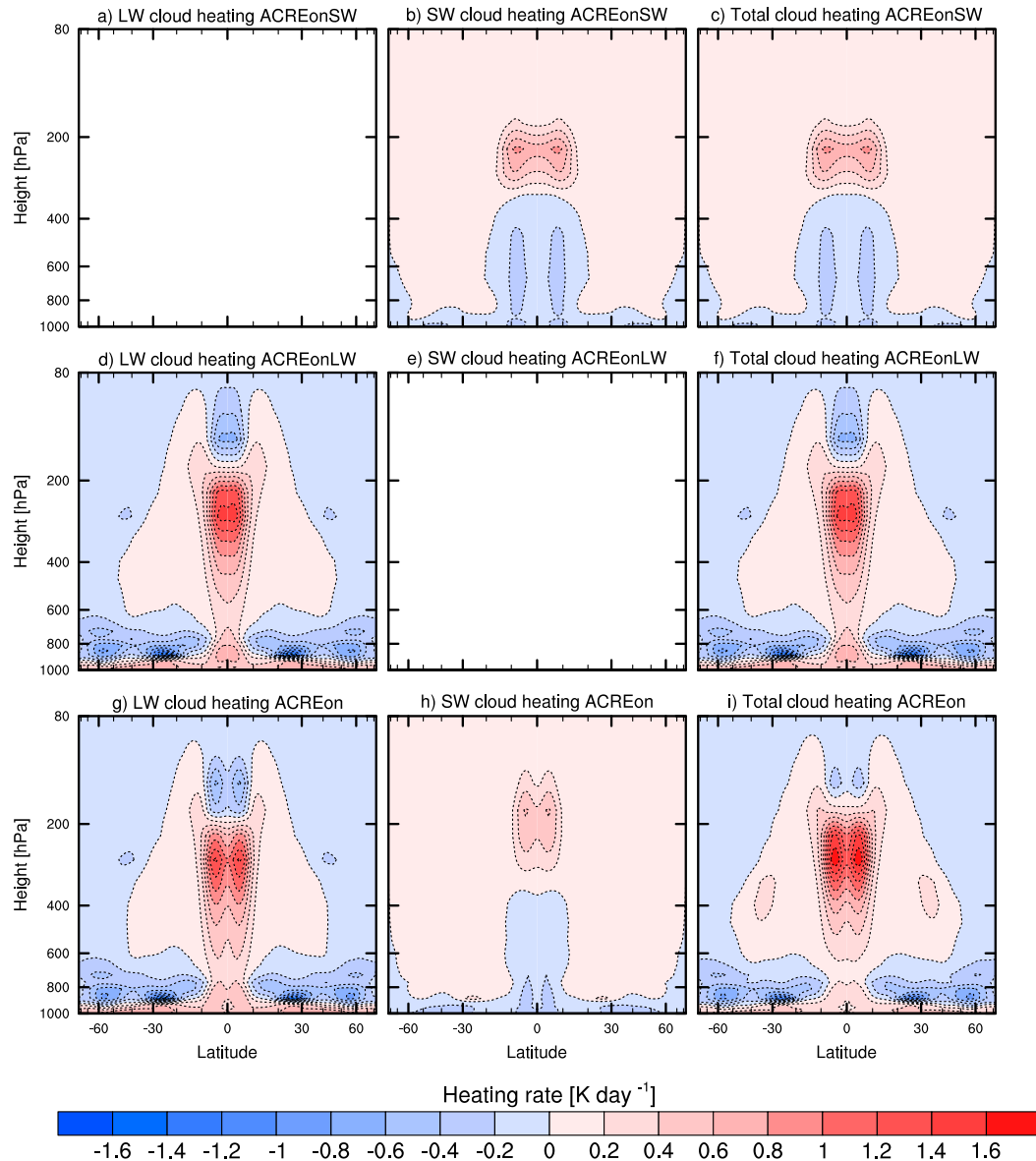
FIG. 3. Zonal-mean cloud-radiative heating rates in steady state: (left) longwave, (center) shortwave, and (right) total (longwave + shortwave) cloud radiative heating, for (a)–(c) ACREonSW, (d)–(f) ACREonLW, and (g)–(i) ACREon. Note, that the horizontal axes are scaled with the cosine of the latitude and that the vertical coordinates are logarithmic.

MSE around the equator increases and narrows with decreasing latitude of the ITCZ (Fig. 5a) and thus also with the increasing strength of convection. Hence the relative width and magnitude of the low-level MSE appear both to be decent predictors of the ITCZ position. This is also the case in all simulations analyzed by Harrop and Hartmann (2016). Note that in our simulations with ACREoff and ACREonSW in which the ITCZ is far from the equator, the meridional MSE distribution is flat around the maximum value at low latitude and the ITCZs tend to lie at the edge of the region of flat meridional MSE. At the 850-hPa level the peaks in MSE are coincidentally located with the ITCZ position and thus explain this effect.

4. An MSE-based mechanism for the ITCZ shift with ACREs

a. Transient simulations

To elucidate how the ACREs affect the low-level MSE we now analyze the transient simulations. All of
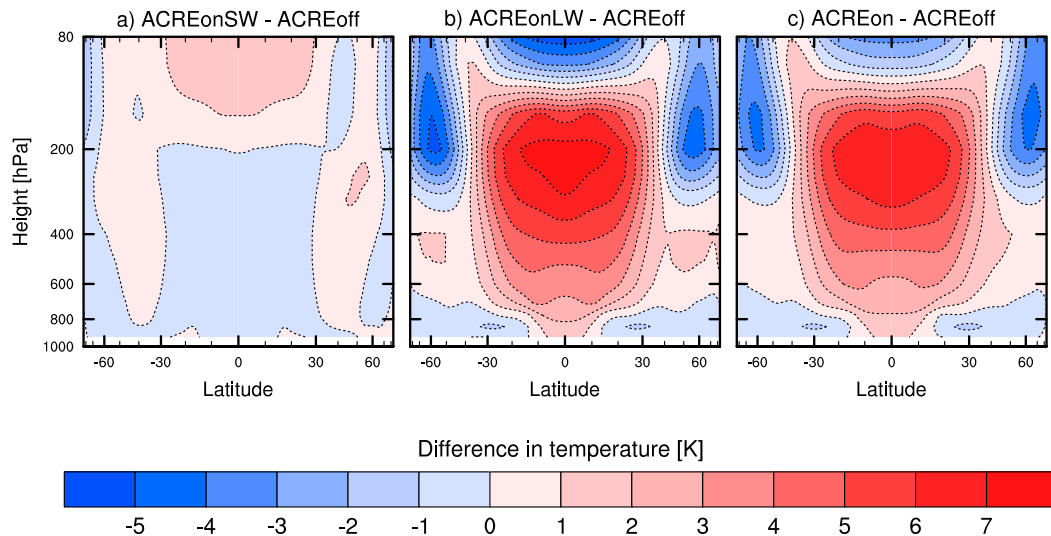
FIG. 4. Difference in steady-state zonal-mean temperature between (a) ACREonSW and ACREoff, (b) ACREonLW and ACREoff, and (c) ACREon and ACREoff. Note that the horizontal axes are scaled with the cosine of the latitude and that the vertical coordinates are logarithmic.

the following analysis is performed using 3-hourly data. We first focus on an ensemble of simulations in which the longwave ACRE is turned on at the beginning of the simulations. It takes around 50 days for the ITCZs to move to the equator and form a single ITCZ (Figs. 6a,d). Therefore we will focus our analysis on this initial period. In the first days of simulation the temperature, specific humidity, and accordingly the MSE increase fastest at around 5.5° latitude and hence equatorward of the original ITCZ position at 8.5° latitude (henceforth denoted as "off the equator") (Figs. 6b,c). As a consequence the ITCZ starts to move toward the equator (Fig. 6d). After 10 days the specific humidity and the MSE increase fastest at the equator (Figs. 6b,c). After 30 days the temperature, specific humidity, and MSE at the equator become larger at the equator than at 5.5° latitude and consequently the ITCZ moves equatorward of 5.5° (Fig. 6d). The MSE does not increase any more at 5.5° latitude after around 30 days and ceases to increase at the equator after around 40 days, coincidentally with the ITCZ reaching the equator. The higher rate of increase in MSE equatorward of the
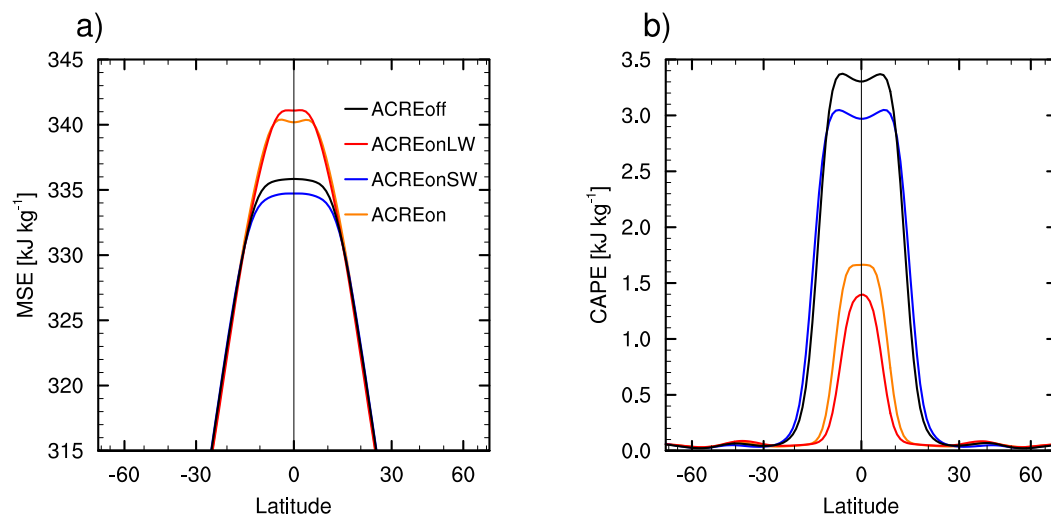

FIG. 5. (a) The steady-state zonal-mean MSE at 925 hPa for ACREoff, ACREonSW, ACREonLW, and ACREon. (b) The steady-state zonal-mean CAPE as a function of latitude for the same experiments. Note that the horizontal axes are scaled with the cosine of latitude.
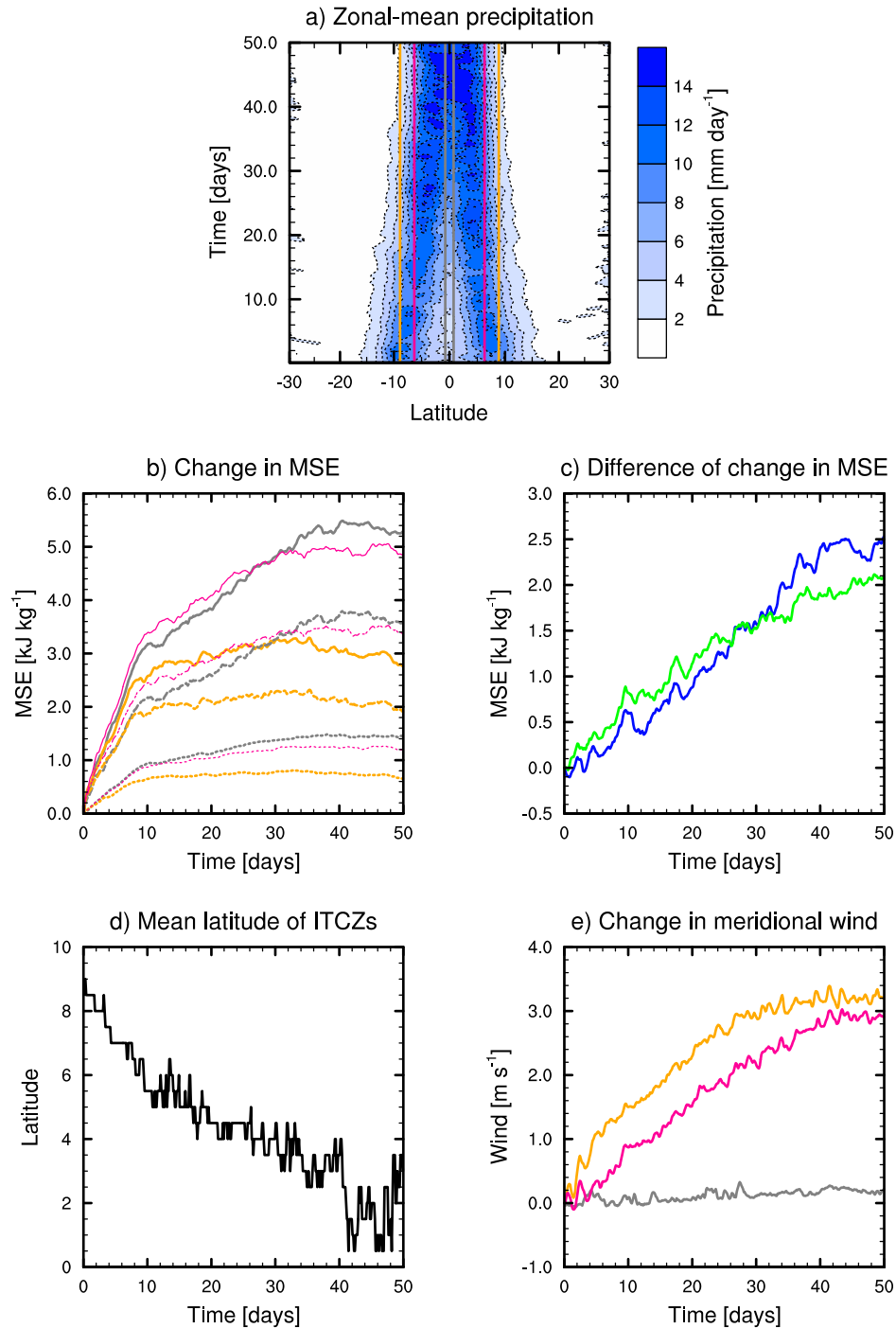
FIG. 6. (a) The zonal- and ensemble-mean total precipitation as a function of latitude and time for the 10-member ensemble of transient simulations starting from steady-state ACREoff conditions with the longwave ACRE abruptly turned on at the start of the simulations. The latitudes of $\pm 0.5°$ are denoted with gray lines, the latitudes of $\pm 5.5°$ with magenta lines, and the latitudes of $\pm 8.5°$ with orange lines. (b) The temporal evolution of the change in MSE (solid) and of the contributions of the specific humidity (dashed) and of the temperature (dotted) to the change in MSE in the same simulations in zonal and ensemble mean at $0.5°$ latitude (gray), $5.5°$ latitude (magenta), and $8.5°$ latitude (orange) averaged over both hemispheres {e.g., $h(\phi_{\mathrm{both}} = 0.5°) = [h(\phi = 0.5°) + h(\phi = -0.5°)]/2$}. (c) The difference in change in MSE between $0.5°$ and $8.5°$ latitude (blue) and between $5.5°$ and $8.5°$ latitude (green) averaged over both hemispheres. (d) The latitude of the ITCZ evaluated as the maximum in ensemble-mean zonal-mean precipitation on average over both hemispheres. (e) The change in zonal- and ensemble-mean meridional wind at 925 hPa at $0.5°$ latitude (gray) $5.5°$ latitude (magenta), and $8.5°$ latitude (orange) averaged over both hemispheres.
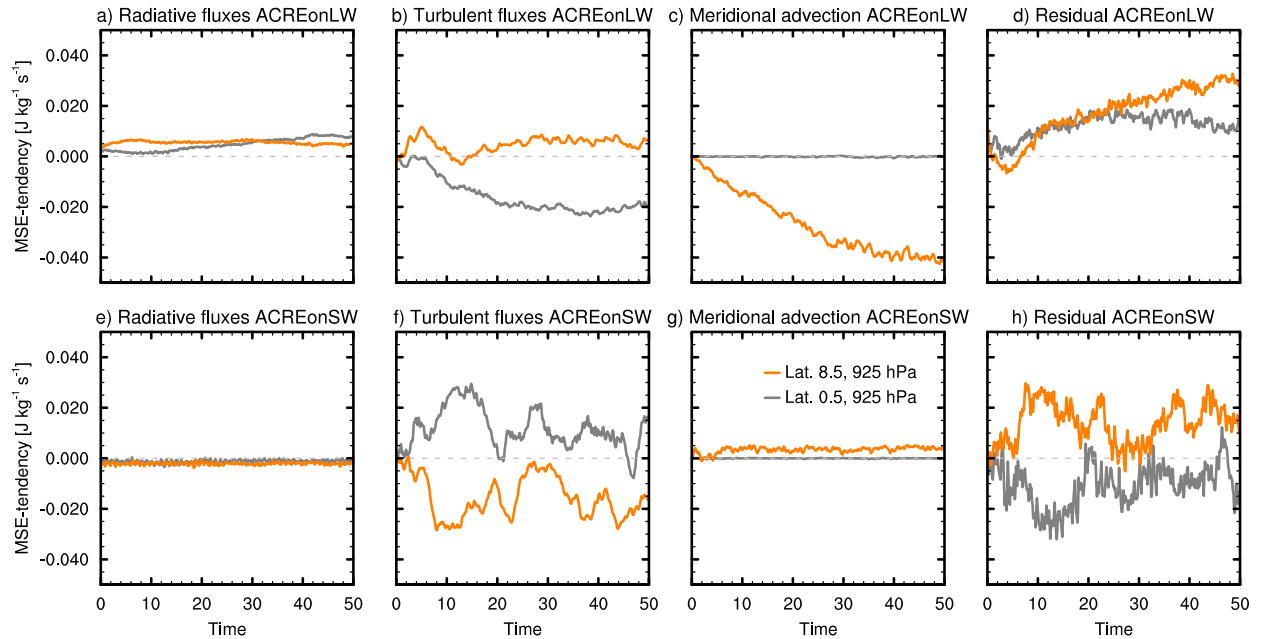
FIG. 7. Temporal evolution of the change in zonal- and ensemble-mean MSE tendencies from the initial state at latitudes 0.5° (gray) and 8.5° (orange) due to (left)–(right) the radiative flux-divergence, the turbulent fluxes at the surface, the zonal-mean meridional advection of MSE, and the residual terms. Results are from the 10-member ensemble of transient simulations starting from steady-state ACREoff conditions with the (a)–(d) longwave or (e)–(h) shortwave ACRE abruptly turned on at the start of the simulations. As in the previous two plots, averages are taken over latitudes on both hemispheres.

original location of the ITCZ and the prolonged increase at the equator are responsible for the larger increase in MSE at the equator than off the equator and thereby for the ITCZ moving to the equator.

b. A mechanism for the ITCZ shift with ACREs

The zonal-mean energy budget can be written as

$$\frac{\overline{\partial h}^{\lambda}}{\partial t} = c_p \overline{R}^{\lambda} + \chi(z)\overline{F_t}^{\lambda} - \frac{1}{a\cos(\phi)}\overline{u\frac{\partial h}{\partial \lambda}}^{\lambda}$$
$$- \frac{1}{a}\overline{v\frac{\partial h}{\partial \phi}}^{\lambda} - \overline{w\frac{\partial h}{\partial z}}^{\lambda} - (c_v - c_p)\frac{\partial \overline{T}^{\lambda}}{\partial t} + \overline{r_n}^{\lambda}, \quad (2)$$

where λ denotes the longitude, ϕ the latitude, z the height over ground, and u, v, and w the zonal, meridional, and upward components of the velocity vector, respectively. The specific heat capacity of air at constant volume is denoted by c_v, the radiative heating by R, the turbulent energy fluxes at the surface by F_t, and the radius of Earth by a. Overbars ($\overline{}^{\lambda}$) denote zonal means. The term $\overline{r_n}^{\lambda}$ is a residual of interpolation errors from postprocessing and from the dissipation of kinetic energy. The function $\chi(z)$ is one when z is zero (at the surface) and is zero for all other values of z. We rewrite Eq. (2) by splitting the advective terms into zonal-mean and eddy contributions and by expressing all terms

except the turbulent fluxes at the surface, the radiative heating term, and the zonal-mean meridional advection as a total residual r_t and obtain

$$\frac{\overline{\partial h}^{\lambda}}{\partial t} = c_p \overline{R}^{\lambda} + \chi(z)\overline{F_t}^{\lambda} - \frac{1}{a}\overline{v}^{\lambda}\frac{\overline{\partial h}^{\lambda}}{\partial \phi} - \overline{r_t}^{\lambda}. \quad (3)$$

How do the four terms on the right-hand side of Eq. (3) affect the total tendency of MSE? The increase in absorption of longwave radiation leads initially to a positive radiative tendency in MSE both on and off the equator of similar magnitude (Fig. 7a). Therefore, it is the response of the other terms that determines the difference in response of the MSE on and off the equator. The turbulent fluxes at the surface decrease at the equator and reduce the MSE tendency (Fig. 7b). The change in the turbulent heat fluxes oscillates around zero off the equator in the first 15 days and then becomes positive (Fig. 7b). Since the larger increase in MSE at the equator does not appear to be caused by local processes, it must be caused by changes in the advective terms and thus by changes in the large-scale circulation, and possibly by the numerical residual. It was shown earlier that the Hadley circulation strengthens when the longwave ACRE is turned on. This strengthening leads to an increase in zonal-mean meridional wind at low levels off the equator (Fig. 6e), whereas it has to remain zero at

the equator for reasons of symmetry. Furthermore, the larger warming at low latitudes due to the longwave heating and the overall warming of the deep-tropical boundary layer also increases the meridional low-level MSE gradient. As a consequence, the zonal-mean equatorward advection of MSE strongly increases off the equator whereas it remains zero at the equator (Fig. 7c). Since the advection of MSE is upgradient, this leads to a strong negative MSE tendency, which counteracts the radiative heating and thus stabilizes the MSE at a lower value off the equator than at the equator (Fig. 6b). The residual term is relatively large (Fig. 7d), suggesting that other terms have sizeable contributions to the total tendency. The increase in horizontal advection of MSE by zonal eddies off the equator contributes to the negative tendency in the first 10 days of the simulation, but decreases thereafter and is less than 10% of the tendency from the advection by the mean flow after 40 days (not shown). The largest contribution to the residual at the end of the 50-day period comes from the vertical advection of MSE and the numerical residual (not shown). However, the change in zonal-mean advection of MSE is by far the largest single change in tendency off the equator and thus largely responsible for countering the initial radiative heating. In summary, we propose that the ITCZ moves toward the equator because the increase in large-scale circulation causes a decrease in the advective tendency for the low-level MSE off the equator and the low-level MSE thus becomes more sharply peaked at the equator.

The mechanism for the ITCZ shift due to the longwave ACRE also occurs with the shortwave ACRE, but in the opposite sense. The shortwave ACRE reduces solar absorption by water vapor both on and off the equator and leads thus to a negative radiative tendency of MSE (Fig. 7e) at low levels. The decrease in vertically integrated shortwave heating at low latitudes (10°S–10°N) is larger than at higher latitudes (around 20°N and 20°S; not shown) and therefore the meridional heating gradient decreases. The decrease in meridional heating gradient leads in turn to a decrease of large-scale circulation and thus to a slowdown of the zonal-mean meridional wind off but not at the equator (Fig. 7g). As a consequence, less MSE is advected off the equator, which leads to a positive change in the tendency of MSE. This positive change counteracts the shortwave cooling and leads to a decrease in MSE that is smaller than at the equator. This contributes to a flattening of the meridional MSE profile at low latitudes and thus to the ITCZ moving farther away from the equator (Fig. 5a). However, other terms like the change in MSE tendency due to the turbulent fluxes are considerably larger in absolute magnitude than that from the zonal-mean

meridional advection off the equator (Fig. 7f). The residual is positive and considerably larger than the change in tendency from the zonal-mean meridional advection (Fig. 7h). The tendencies from the meridional advection by eddies and from the vertical advection are of about the same magnitude and sign as the tendencies from the zonal-mean meridional advection (not shown). The remainder of the residual is due to the numerical residual.

The mechanism introduced above, by which changes in the Hadley circulation influence the advection of MSE and thereby lead to different responses in MSE on and off the equator, only accounts for ACREs through the changes in heating/cooling rates. In principle, this mechanism could therefore be applicable to other perturbations of the atmospheric energy balance. Oueslati and Bellon (2013b) found a similar feedback mechanism by which an increased large-scale circulation increases the advection of colder air more off than at the equator when studying the influence of meridional SST gradients on the ITCZ position. Since colder air contains less water vapor at the same relative humidity and since the relative humidity tends to be lower in the subtropics, the advection of colder and drier air from the subtropics corresponds to the advection of air with lower MSE. In this regard, despite the different forcings and approach by Oueslati and Bellon (2013b), the mechanisms by which the ITCZ moves toward the equator are similar in the two studies. The ''upped ante'' mechanism (Neelin et al. 2003), by which larger horizontal gradients of moisture in a warmer climate increase the advection of dry air into the margins of tropical convective regions, thereby reducing convection in the margins, is similar to our mechanism in that increased advection of air of low MSE suppresses convection. However, in our simulations the key is an increased large-scale circulation whereas the key of the upped-ante mechanism is an increased MSE gradient.

c. The relation between the position and the width of the ITCZ

Our results suggest that the distribution of precipitation around the equator narrows as the ITCZs move toward the equator. This is consistent with the behavior of other models (Harrop and Hartmann 2016). Byrne and Schneider (2016b) show that total top-of-the-atmosphere cloud-radiative effects (CREs) affect the width of the ITCZ in climate change experiments. This raises two questions: Are the width and the position of the ITCZ linked, and are they controlled by similar mechanisms? Byrne and Schneider (2016a) suggest that a narrowing of the upwelling region of the Hadley circulation is consistent with an increased contribution
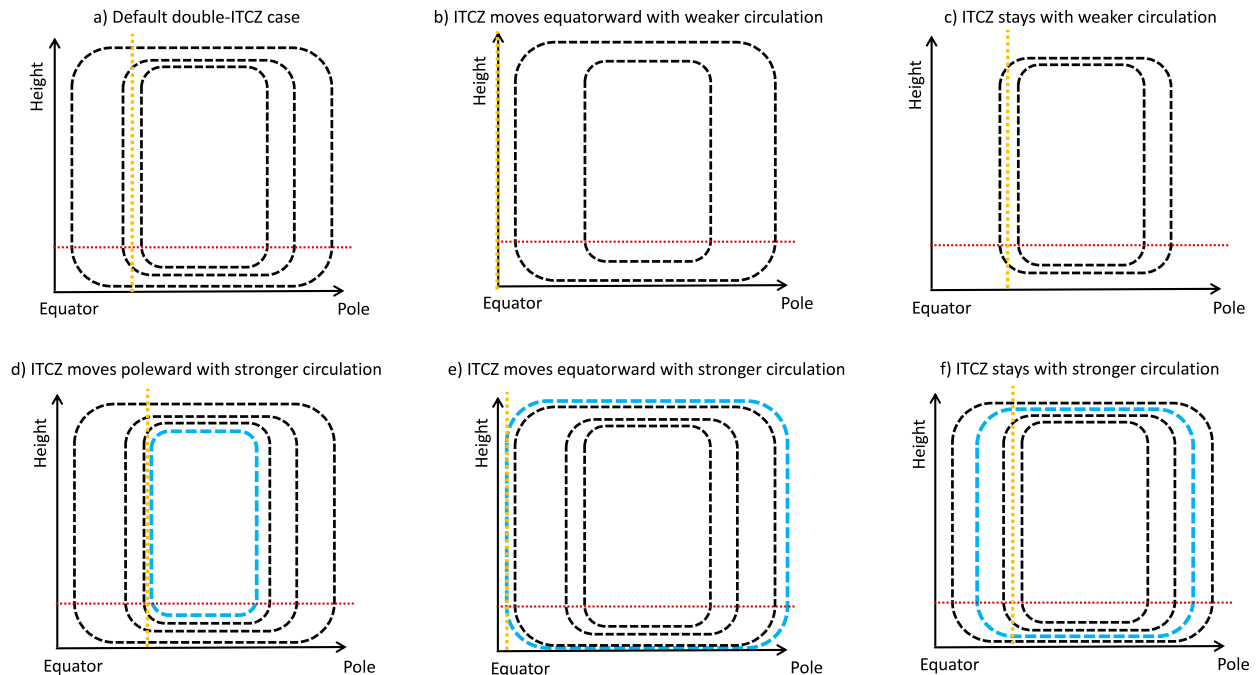
FIG. 8. Sketches of the Eulerian zonal-mean mass streamfunction in different hypothetical cases. Contours always are equally spaced and the circulation is clockwise. Wind speeds are highest were the streamlines are densest. Thus, the ITCZs are the locations (indicated by orange lines) where the vertical streamlines are densest on the equatorward side of the Hadley cell. The total strength of the Hadley circulation corresponds to the total number of streamlines. The horizontal red line indicates the top of the boundary layer. We sketch five different changes in Hadley circulations from (a) the default double-ITCZ case by leaving or adding extra streamlines (in blue). Adding streamlines corresponds to a strengthening of the Hadley circulation and removing to a weakening. We thus show that without further mechanisms to constrain possible changes the ITCZ can move equatorward with a (b) weaker or (e) stronger circulation than in the default case, that it may stay with a (c) weaker or (f) stronger circulation, and that (d) it can move poleward with a stronger circulation. Thus, the strength of the Hadley circulation alone does not constrain the position of the ITCZ.

to the tropical atmospheric energy uptake from that region. This mechanism causes the strengthening of the Hadley circulation and thus the ITCZ to move toward the equator in our simulations as well. Furthermore, Byrne and Schneider (2016b) find that an increase in zonal-mean meridional advection of MSE contributes to a narrowing of the ITCZ in climate change experiments. This mechanism is similar to the one we suggest to be responsible for the ITCZ moving toward the equator with the difference that the change in meridional MSE gradient is key for the change in MSE advection in Byrne and Schneider (2016b) whereas the acceleration of the meridional wind is key in our study. So the processes that govern the width of the ITCZ and the position of the ITCZ appear to be related. The width but not the position of the ITCZ is also influenced by the MSE advection by the eddies (Byrne and Schneider 2016b). This either could be due to the poleward margins of the ITCZ being at higher latitude than the peaks where eddies tend to play a larger role in the energy transport or could be due to the differences in experimental setups. A detailed analysis of this would go

beyond the scope of our discussion, and is therefore left to future studies.

d. The relation between the strength of the Hadley circulation and the ITCZ position

Does a strengthening of the Hadley circulation trivially lead to the ITCZ position moving toward the equator? From a circulation standpoint alone, this is certainly not the case. We can illustrate cases with weaker large-scale circulation and an ITCZ closer to the equator (Fig. 8) or conversely a stronger large-scale circulation with the ITCZ farther away from the equator (Fig. 8). This is because the location of the ITCZ is where the low-level convergence of $\bar{v}^\lambda$ is largest, irrespective of the magnitude of $\bar{v}^\lambda$. Therefore, we require the additional energetic argument of the different changes in MSE advection on and off the equator to explain why the magnitude of $\bar{v}^\lambda$ influences the latitude at which the low-level $\bar{v}^\lambda$ will maximize.

In principle, any strengthening of the Hadley circulation leads to a larger increase of MSE advection off the equator than at the equator, because any strengthening

of the Hadley circulation leads to an increase of $\overline{v}^\lambda$ off the equator (at least vertically integrated over low levels). This mechanism favors the ITCZ to move toward the equator, but whether the ITCZ actually moves equatorward depends on whether this is the leading mechanism. In our simulations this is the case, because 1) the SSTs are prescribed and 2) the imposed forcing leads to an increase in atmospheric energy uptake. Reason 1 prevents a strong thermodynamic readjustment of the atmosphere that may either change the efficacy of the energy transport or change the radiative fluxes such that the meridional gradient in energy uptake is reduced. Reason 2 ensures that the changes in turbulent fluxes do not dominate the changes in MSE advection off the equator. An increase in near-surface winds consistent with an increase in large-scale circulation would act to reduce the meridional gradient in atmospheric energy uptake by increasing the turbulent fluxes at the surface more off than at the equator. However, this would lead to an additional increase of the net energy input into the atmosphere, and would thus push the atmosphere even more away from a steady state. In a scenario with an increased meridional gradient in atmospheric energy uptake but a decreased overall atmospheric energy uptake in the tropical mean, the change in turbulent fluxes could be the main mechanism balancing the meridional energy gradient. In this case, the ITCZ would not necessarily move toward the equator despite an increase in large-scale circulation. So in summary, the proposed mechanism favors the ITCZ to move toward the equator with a strengthening of the meridional overturning circulation, but whether the ITCZ actually moves depends on the experimental setup.

5. Previous frameworks for interpreting changes in ITCZ position

a. Atmospheric stability and CAPE

As one of the motivations for using the low-level MSE, we mentioned that the mean meridional gradient of the upper-tropospheric MSE is small in the tropics. However, the value of mean MSE in the upper troposphere may change between experiments and thus the mean atmospheric stability may change as well. In agreement with previous work (Harrop and Hartmann 2016), we find that the net ACRE has an increasing warming effect with height in the tropics (Fig. 4c). This suggests that the mean stability of the atmosphere is higher when ACREs are turned on. A way of measuring the stability of the atmosphere is CAPE. Smaller values of CAPE tend to indicate a more stable atmosphere. Consistent both with an increase in mean static stability

and with most previous results, we find that the mean CAPE is indeed considerably smaller in the ACREon than in the ACREoff experiments and also has a narrower distribution around the equator (Fig. 5b). Landu et al. (2014) suggest that a decrease in mean CAPE could cause an equatorward shift of the ITCZs, because a reduction of mean CAPE would make the atmosphere more stable, such that convection only occurs where the SSTs are highest around the equator. So this mechanism suggests that the changes in stability induced by the ACREs directly cause the ITCZ position to change, whereas our mechanism suggests that the strengthening of the large-scale circulation as a response to the ACREs drives the change in ITCZ position. The mechanism based on the reduction of CAPE does not, however, explain our ACREonSW experiment, which has a smaller peak of mean CAPE than the ACREoff experiment but whose ITCZ is farther away from the equator. It is also noteworthy that Harrop and Hartmann (2016) find that the mean CAPE is even larger in the ACREon experiment with the CNRM model, even though the ITCZs lie closer to the equator in that case. So in at least two simulations the reduction of CAPE cannot explain the shift in ITCZ position whereas our MSE framework explains the change in ITCZ position consistently in all simulations. This suggests that the reduction of mean CAPE that occurs in most simulations when cloud-radiative effects are turned on could be an effect of the changes in convection in these particular models. So while CAPE is a useful quantity for many purposes, the shift of the ITCZ due to ACREs is better described by the MSE mechanism illustrated here.

b. A gross-moist-stability perspective

1) A GROSS-MOIST-STABILITY FRAMEWORK

We showed in the last subsection that the ACREs affect not only the position of the ITCZ but also the mean atmospheric stability. The mechanism we propose for the change in position of the ITCZ by the ACRE only takes changes of the low-level MSE into account, because the upper-tropospheric MSE is nearly constant in the tropics in each of the simulations. However, the magnitude of the precipitation may well depend on how the stability changes in the upper troposphere between simulations. A framework to understand this interaction between the atmospheric stability, the heating of the atmosphere, and the large-scale circulation has been developed by Neelin and Held (1987). The framework is based on the observation that the mean horizontal mass transport consists of a low-level flux toward regions of low pressure and a flux of same magnitude but opposite

direction in the upper level. The net energy transport is then equal to the difference in energy per mass transported by the two branches of the circulation. In steady state the net energy-flux divergence has to balance the atmospheric energy uptake. The vertically integrated zonal-mean energy balance in steady state can thus be written as

$$-\frac{1}{a}\left[\frac{\partial}{\partial\phi}+\tan(\phi)\right](\Delta h\langle\overline{v}^{\lambda,t}\rangle_{p_l}) = \overline{A}^{\lambda,t}, \qquad (4)$$

where A is the atmospheric energy uptake and v the meridional wind. Overbars ($\overline{}^{\lambda,t}$) denote zonal and temporal means. Angle brackets denote the mass-weighted vertical integral over the entire depth of the atmosphere (p) or over the depth of the lower branch (p_l). The quantity Δh corresponds to the amount of energy transported per unit mass and can be expressed following Kang et al. (2009) as

$$\Delta h = -\frac{\langle\overline{hv}^{\lambda,t}\rangle_p}{\langle\overline{v}^{\lambda,t}\rangle_{p_l}}. \qquad (5)$$

The term Δh is commonly referred to as a gross moist stability; it gives an indication of the energy transport and a rough estimate of the atmospheric stability. If Δh is known, Eq. (4) can be used to infer $\langle\overline{v}^{\lambda,t}\rangle_{p_l}$. Assuming no eddy transport of moisture and neglecting the moisture transport by the upper branch, the lower-level mass flux can be used to infer the local moisture convergence (Kang et al. 2009):

$$\frac{1}{a}\left[\frac{\partial}{\partial\phi}+\tan(\phi)\right](\overline{q}_l^{\lambda,t}\langle\overline{v}^{\lambda,t}\rangle_{p_l}) = \overline{P}^{\lambda,t} - \overline{E}^{\lambda,t}, \qquad (6)$$

where q_l is the lower-level specific humidity, P is the precipitation, and E is the evaporation. Since the evaporation varies much less with latitude than the precipitation does in the deep tropics, the right-hand side can be used to give an approximation of the ITCZ position. This framework is especially attractive to study changes in ITCZ position in the context of ACREs because we can directly apply the cloud-induced changes in the radiative fluxes to estimate changes in the ITCZ position.

Recently a variation of the gross moist stability framework has been used (Fläschner 2016) in which the gross moist stability is used to infer the mean vertical velocity (e.g., Neelin and Zeng 2000; Back and Bretherton 2006; Raymond et al. 2009). While this framework gives an accurate prediction of the ITCZ position (Fläschner 2016), it requires the prescription of the mean horizontal advection to infer the vertical

velocity and is therefore less well suited for the task at hand than the framework we use here.

2) PREDICTION OF THE ITCZ POSITION WITH THE GROSS-MOIST-STABILITY FRAMEWORK

We test the ability of the gross-moist-stability framework to predict the position of the ITCZ as follows. We assume that Δh does not change between simulations, implying a constant atmospheric stability. We estimate Δh by fitting a fourth-order polynomial to the Δh calculated from our simulations (Fig. 9a). By applying the model output from our simulations for $\overline{A}^{\lambda,t}$ and our fit of Δh to Eq. (4) we calculate $\langle\overline{v}^{\lambda,t}\rangle_{p_l}$. The thus obtained $\langle\overline{v}^{\lambda,t}\rangle_{p_l}$ and the model output from our simulations for $\overline{q}_l^{\lambda,t}$ are then applied to Eq. (6) to calculate $\overline{P}^{\lambda,t} - \overline{E}^{\lambda,t}$ (Fig. 9b).

Despite some differences in the maximum and minimum values, the thus predicted $\overline{P}^{\lambda,t} - \overline{E}^{\lambda,t}$ is qualitatively similar to that in our simulations, especially in that the longwave ACRE draws the ITCZ toward the equator whereas the shortwave ACRE draws it poleward (Figs. 9b and 10a). Hence the ITCZ position changes without a change in mean moist stability. However, the transition to a single ITCZ is not reproduced. This is due either to our particular choice of gross moist stability or to the neglect of the moisture transport by eddies. If we replace Δh in all our simulations by the Δh of the ACREonLW experiment (with the single ITCZ), the gross-moist-stability framework yields a single ITCZ (not shown). This means that the failure to reproduce a single ITCZ is mostly caused by our choice of Δh. The gross-moist-stability framework also suggests that the predicted evaporation exceeds the predicted precipitation at the equator in the ACREoff and ACREonSW simulations whereas it does not in the actual simulations. This stems from choosing Δh to be strictly positive (for numerical reasons), whereas it is negative close to the equator in these two simulations. So it appears that changes in stability have an influence on the ITCZ position right at the equator where Δh is small and thus most sensitive to errors, whereas changes in stability hardly affect the ITCZ position anywhere else. However, the stability has a large influence on the amount of precipitation in the deep tropics (not shown).

3) CONTRIBUTIONS OF CHANGES IN RADIATIVE, TURBULENT FLUXES, AND HUMIDITY TO THE CHANGES IN ITCZ POSITION

Since the gross-moist-stability framework can qualitatively predict the ITCZ position, we can ask how other factors like changes in turbulent surface fluxes, changes in radiative heating, or changes in humidity affect the position of the ITCZ in this framework. We apply again
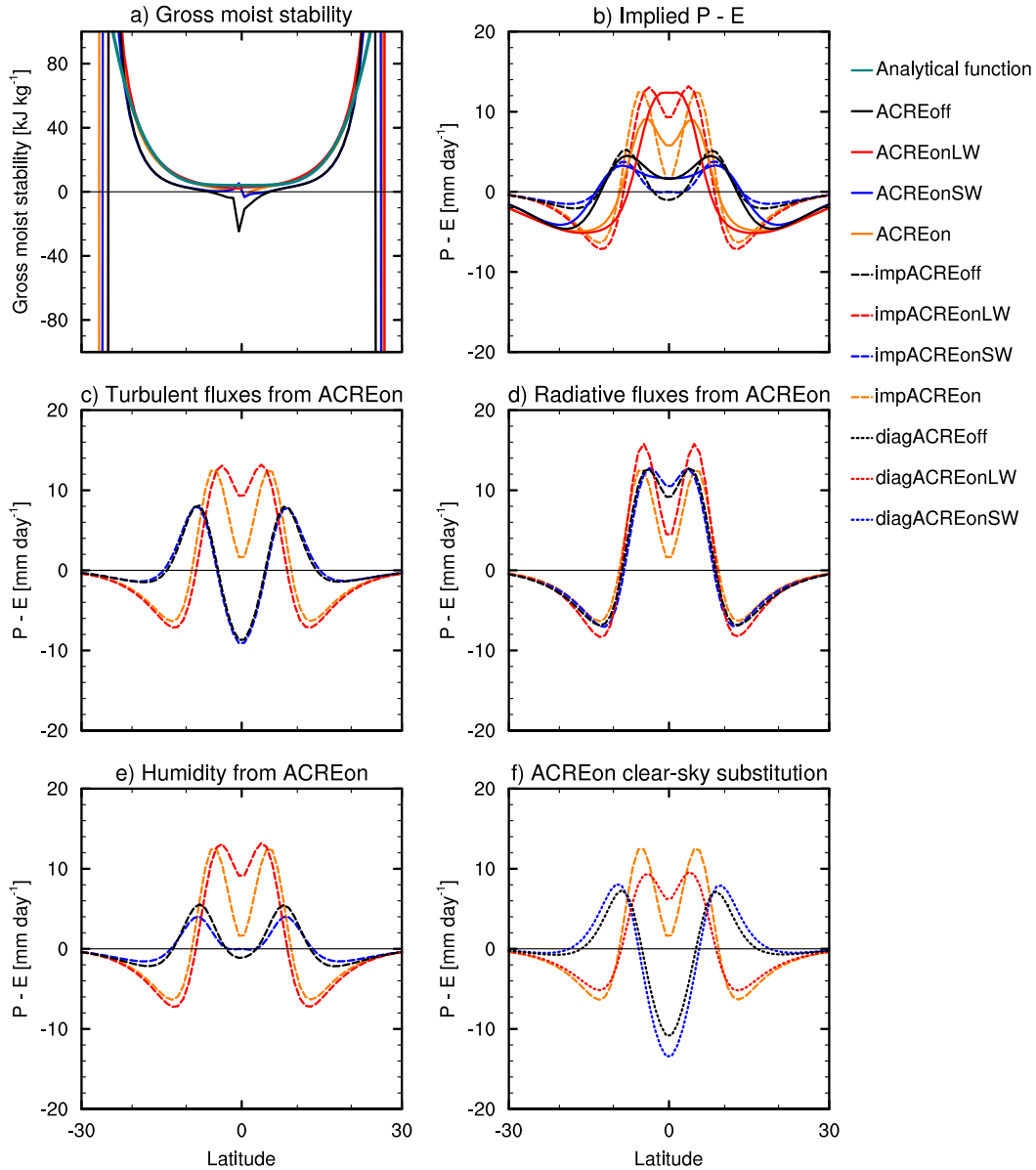
FIG. 9. (a) The zonal-mean gross moist stability calculated from the model output as well as the analytical function used to approximate the gross moist stability (turquoise line) as a function of latitude. (b) The implied $\overline{P}^{\lambda,t} - \overline{E}^{\lambda,t}$ obtained with the gross-moist-stability framework (dashed lines) and $\overline{P}^{\lambda,t} - \overline{E}^{\lambda,t}$ from the model output (solid lines) as a function of latitude. The inferred $\overline{P}^{\lambda,t} - \overline{E}^{\lambda,t}$ under the assumptions, respectively, that (c) the turbulent fluxes are the same as in ACREon in all four experiments, that (d) the radiative fluxes are the same as in ACREon in all four experiments, and that (e) the specific humidity is the same as in ACREon in all four experiments. (f) The inferred $\overline{P}^{\lambda,t} - \overline{E}^{\lambda,t}$ when the longwave fluxes from the ACREon experiment are replaced by the clear-sky longwave fluxes from the same experiment (diagACREonSW), when the shortwave fluxes from the ACREon experiment are replaced by the clear-sky shortwave fluxes from the same experiment (diagACREonLW), and when both fluxes from the ACREon experiment are replaced by the clear-sky fluxes from the same experiment (diagACREoff). Note that the horizontal axes are all scaled with the cosine of latitude.

the polynomial fit of Δh to all simulations (Fig. 9a), implying no change in moist stability between experiments. By allowing only the quantity of interest to change, we find that the changes in radiative cooling

together with the implied changes in circulation explain most of the changes in ITCZ position (cf. the ITCZ positions in Figs. 9d and 9b, and see Fig. 10a), whereas the changes in turbulent fluxes (cf. the ITCZ positions in
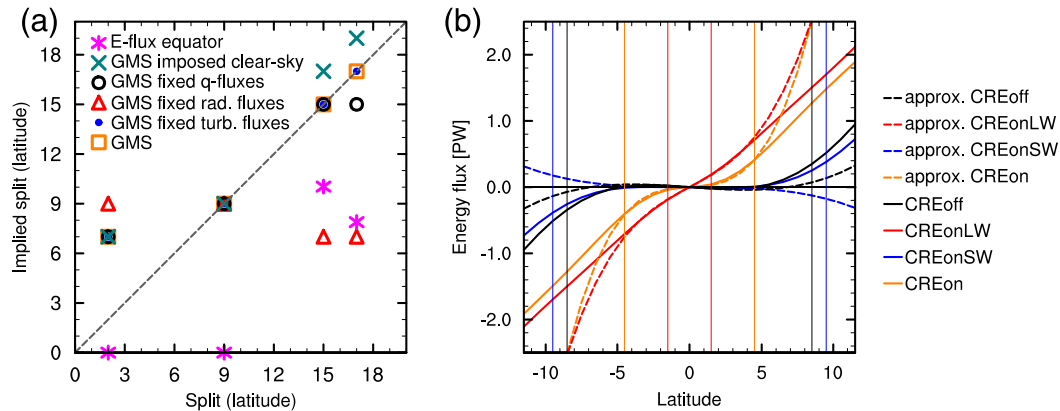
FIG. 10. (a) The implied split in latitude between the two ITCZs [as defined in Popp and Lutsko (2017)], as a function of the actual split between the two ITCZs in the four experiments. In the hemispherically symmetric setup used here, the split should approximately correspond to twice the distance of each of the ITCZs from the equator. In a perfect prediction the implied split by a certain framework would be equal to the simulated split and would thus lie on the gray dashed line. The splits of the actual simulations are 2° (ACREonLW), 9° (ACREon), 15° (ACREoff), and 17° (ACREonSW) latitude. The marks shown are for the energy-flux framework [magenta asterisks; see (b)], the gross-moist-stability (GMS) framework (orange squares; Fig. 9b), and the GMS framework with fixed turbulent fluxes (blue dots; Fig. 9c), with fixed radiative fluxes (red triangles; Fig. 9d), with fixed specific humidity (black circles; Fig. 9e), and with the all-sky fluxes replaced by the clear-sky fluxes (turquoise crosses; Fig. 9f). (b) The vertically integrated zonal-mean meridional energy flux as a function of latitude (solid) and a third-order Taylor expansion thereof (dashed) following the approach by Bischoff and Schneider (2016). The vertical lines denote the ITCZ positions according to the zonal-mean precipitation maxima in our simulations.

Figs. 9c and 9b, and see Fig. 10a) and humidity (cf. the ITCZ positions in Figs. 9e and 9b, and see Fig. 10a) and their implied changes to the circulation have almost no influence on the ITCZ position. A previous study found that imposed changes in the entrainment rate of deep convection could change the ITCZ position by changing the turbulent fluxes at the surface (Möbis and Stevens 2012). This effect may have a small influence on the ITCZ position, but is apparently not the main effect that changes the ITCZ position when changes in ACREs are driving the changes.

4) CAN CHANGES IN ITCZ POSITION BE PREDICTED FROM THE ACREON EXPERIMENT ALONE?

Using the gross-moist-stability framework, we perform the same analysis as previously, but instead of using the fluxes and humidity from the ACREoff experiment we use the fluxes and humidity from the ACREon experiment and replace the all-sky fluxes by the clear-sky fluxes. Similarly, to mimic the ACREonLW experiment, we replace the shortwave all-sky fluxes by the clear-sky fluxes and mimic the ACREonSW experiment by only replacing the longwave all-sky fluxes by the clear-sky fluxes. This analysis shows that the qualitative change in ITCZ position due to the ACREs can be directly inferred with this approach (cf. Figs. 9f and 9b, and see Fig. 10a). However, correctly predicting the

magnitude of $\overline{P}^{\lambda,t} - \overline{E}^{\lambda,t}$ requires the dynamical response of the atmosphere. This full dynamical response is captured by the interactive ACREonLW, ACREonSW, and ACREoff experiments, which are the focus of the present paper.

5) COMPARISON BETWEEN THE GROSS-MOIST-STABILITY FRAMEWORK AND THE LOW-LEVEL MSE FRAMEWORK

In both the gross-moist-stability and the low-level MSE frameworks the ITCZ responds to the longwave cloud-radiative heating of the deep-tropical troposphere by a strengthening of the large-scale circulation. However, the low-level MSE budget [Eq. (2)] does not involve the horizontal divergence that is used in the gross-moist-stability framework [Eq. (4)] because the horizontal divergence cancels with the vertical divergence and the local mass tendency when mass is conserved. The horizontal divergence term corresponds to a local change in energy because the horizontal circulation removes or adds mass (of nonzero energy) at that location. The horizontal advection term corresponds to a local change in energy because a fraction of the local air is replaced by air that contains a different amount of energy (without locally changing the mass of air). To estimate the importance of the meridional advective term relative to the divergence term, we decompose the left-hand side of Eq. (4) into the two terms:
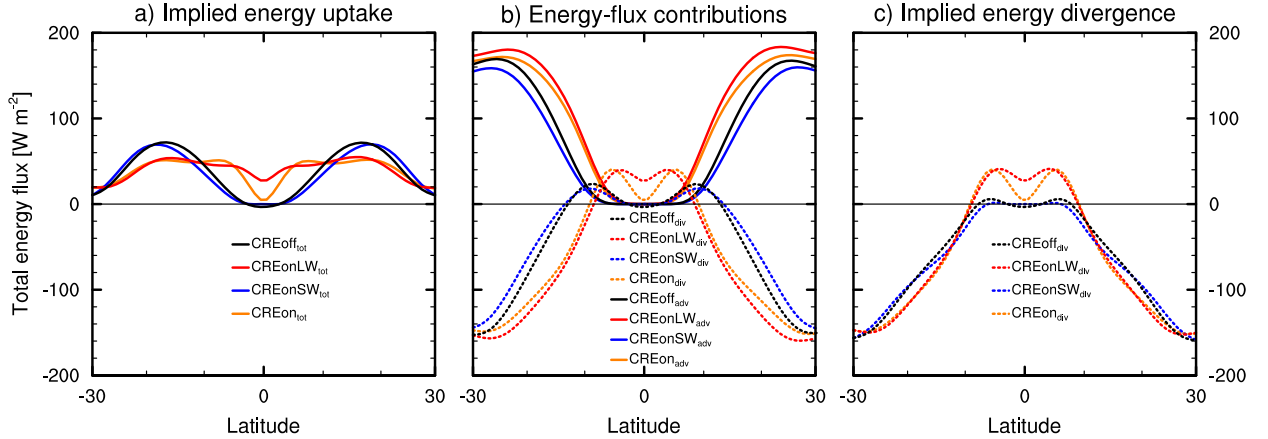
FIG. 11. (a) The implied energy uptake by the atmosphere obtained by evaluating the left-hand side of Eq. (7) using the analytical fit (Fig. 9a) for the gross-moist stability. (b) The divergence (dotted) and the advective (solid) terms in Eq. (7). (c) The implied divergence term obtained, if we subtract the advective term of the ACREon experiment from the implied energy uptake shown in (a) for all four experiments.

$$-\Delta h \frac{1}{a}\left[\frac{\partial}{\partial \phi} + \tan(\phi)\right]\underbrace{\langle \overline{v}^{\lambda,t}\rangle_{p_l}}_{\text{divergence term}} - \underbrace{\frac{1}{a}\frac{\partial \Delta h}{\partial \phi}\langle \overline{v}^{\lambda,t}\rangle_{p_l}}_{\text{advective term}} = \overline{A}^{\lambda,t}.$$

(7)

Assuming again the polynomial fit of Δh for all simulations, we compute $\langle \overline{v}^{\lambda,t}\rangle_{p_l}$ from Eq. (4). The thus obtained $\langle \overline{v}^{\lambda,t}\rangle_{p_l}$ can then be used to calculate the advective and the divergence terms (Fig. 11b). The advective term has a large contribution to the total implied energy transport (Figs. 11a,b). Furthermore, we find that the advective term is more sharply peaked around the equator, the closer the ITCZ is to the equator. This is consistent with the mechanism by which the increase in large-scale circulation causes a decrease in the advective tendency of the low-level MSE and thus the low-level MSE becomes more sharply peaked at the equator, leading in turn to the ITCZ lying closer to the equator. To show this more clearly we recalculate the divergence term by subtracting the advective term of the ACREon experiment from the total implied energy transport shown in Fig. 11a and find that the maxima are then all located at the same position (Fig. 11c). Since the different low-level moisture fields in the different experiments do not appear to affect the location of the ITCZ (Fig. 9e) and since we prescribe the same gross moist stability in the four experiments, this implies that without change in the advective terms, the ITCZ position would hardly change between the experiments.

c. Energy flux perspective

Modeling work suggests that the position of the ITCZ changes as a function of the cross-equatorial energy flux

and thus of the latitude where the vertically integrated zonal-mean meridional energy flux (henceforth called meridional energy transport) vanishes (e.g., Broccoli et al. 2006; Kang et al. 2008; Donohoe et al. 2013). Bischoff and Schneider (2014) and Bischoff and Schneider (2016) have made use of the idea to develop a framework that relates the departure of the ITCZ from the equator to the cross-equatorial meridional energy transport and the deep-tropical atmospheric energy uptake. As in the gross-moist-stability framework, this energy-flux framework starts from the vertically integrated and zonally averaged energy balance, but instead of using the low-level mass flux to infer the ITCZ position, it links the ITCZ position to where the meridional energy transport changes sign and hence direction. To apply their theory to our results we calculate the meridional energy transport $\langle \overline{F_h}^{\lambda,t}\rangle_p$ as

$$\langle \overline{F_h}^{\lambda,t}\rangle_p = 2\pi a \cos(\phi)\langle \overline{hv}^{\lambda,t}\rangle_p$$
$$= \int_0^{\phi'=\phi}\int_0^{2\pi} \overline{A}^t \cos(\phi')a^2 d\lambda\, d\phi'. \quad (8)$$

The overbar ($\overline{}^t$) denotes the temporal mean. This approach correctly predicts two ITCZs in the simulations in which the longwave ACRE is turned off and one ITCZ in the ACREonLW experiment (Fig. 10). However, the zero crossing of the meridional energy transport in the ACREon experiment is at the equator, which would suggest a single ITCZ, whereas we find two ITCZs in our simulations. Furthermore the positions of the ITCZs are located too close to the equator in the experiments with the longwave ACRE turned off.

In our simulations the zero mass streamfunction remains at the equator and thus only coincides with the

ITCZ position in the ACREonLW experiment (Fig. 2). In the ACREon simulation, the transported MSE is larger in the upper branch of the Hadley circulation than in the lower branch, and thus the energy uptake remains positive at the equator (Fig. 1c). Since this means that the energy flux is a monotonically increasing function of latitude, there can only be one energy flux equator (but nonetheless two ITCZs). In the ACREonSW and ACREoff simulations the atmospheric energy uptake becomes negative near the equator (Fig. 1c), whereas the zero mass streamfunction remains at the equator. This means that the lower branch of the Hadley circulation is transporting more energy than the upper branch in this region (Fig. 2). A similar behavior has also been found by Byrne and Schneider (2016a). In this case the location of zero meridional energy transport is linked to where the low-level MSE equals the upper-level MSE rather than to where the meridional gradient of the streamfunction and hence the upward vertical motion is largest. Therefore, the position of zero meridional energy transport does not give accurate approximations of the ITCZ position in these simulations. The net import of energy at the equator from higher latitudes by the large-scale circulation could be an artifact of our model setup, but scenarios where the tropical large-scale circulation imports energy occur in the Pacific in regions of shallow circulations (Back and Bretherton 2006) and are therefore plausible.

6. Implications and conclusions

Many of the models taking part in the CMIP5 experiments exhibit two strong ITCZs in the eastern Pacific too frequently (Li and Xie 2014). A recent study has shown that the hemispherically symmetric component of model biases in precipitation, with which a double ITCZ can be associated, is anticorrelated with the atmospheric energy uptake in the deep tropics (Adam et al. 2016). This is in good agreement with our results, in which the simulations with less deep-tropical energy uptake are the ones with the ITCZ farther away from the equator. The results in Adam et al. (2016) also suggest that the total (top of the atmosphere) CRE in the CMIP5 models is smaller than in observations. If ACREs and CREs affect the ITCZ in a similar way, this would be consistent with a preference for a double ITCZ in our framework and thus with our results. Too small a CRE could be caused by too small a longwave CRE or too large a (negative) shortwave CRE, which both favor ITCZs farther away from the equator according to our simulations. The tropical shortwave CRE bias is larger than the longwave bias in both CMIP and AMIP simulations [see Fig. 7b in Li and Xie (2014)]. If ACRE and

CRE affect the ITCZ in a similar way, then these results and the less pronounced double ITCZ in the AMIP than in the CMIP simulations are consistent with the shortwave CRE being responsible for the bias according to our framework. A too strong shortwave ACRE leads to a poleward shift of the ITCZ in our simulations (as seen as well in the AMIP simulations). Furthermore, the shortwave CRE interacts with the surface energy balance (where its effect is largest) in the CMIP but not in the AMIP simulations. Therefore, we would expect larger biases in the ITCZ position in CMIP than in the AMIP simulations for a similar shortwave CRE bias, whereas a similar longwave CRE bias should result in approximately the same bias in ITCZ position in CMIP and AMIP simulations.

To conclude, we have demonstrated with a state-of-the-art atmospheric GCM that ACREs have a large influence on the tropical large-scale circulation and in particular on the position of the ITCZ. The longwave ACRE pulls the ITCZ toward the equator, thereby substantially reducing the double ITCZ found in simulations with ACREs turned off. By contrast, the shortwave ACRE pushes the ITCZ away from the equator. In our simulations the longwave ACRE has a stronger influence on the ITCZ than the shortwave ACRE does. We have introduced a mechanism to explain these shifts in ITCZ position as a result of ACREs. The mechanism is as follows. The ACREs enhance the atmospheric energy uptake in the deep tropics. This causes the Hadley circulation to respond by strengthening in order to export more energy away from the tropics. This circulation strengthening leads to an acceleration of the low-level zonal-mean meridional wind off the equator and thereby to a negative tendency in low-level MSE due to the increased upgradient advection of MSE. This negative tendency is absent at the equator because the zonal-mean meridional wind is constrained to remain zero at the equator because of the hemispheric symmetric experimental setup. Therefore, the peak of low-level MSE and hence the ITCZ move equatorward. Changes in turbulent surface fluxes appear to play only a minor role in driving the change.

Our framework based on gross moist stability suggests that the ACREs diagnosed from a single simulation are sufficient to predict the qualitative response of the ITCZ to changes in ACREs, but that additional experiments similar to the ones here are necessary in order to infer the change in the amount of precipitation due to the ACREs. Our results suggest, furthermore, that the energy-flux framework yields inaccurate predictions of the ITCZ position if there is a change in sign of the gross moist stability far away from the zero mass streamfunction, or if the maximum

upward vertical velocities do not coincide with the zero mass streamfunctions.

By tinkering with the interaction between clouds and radiation we have demonstrated the importance of ACREs to the ITCZ and developed a physical mechanism that explains how the ACREs influence the circulation, the energetics, and the resultant precipitation. In addition, we have compared and contrasted several different frameworks that have previously been used to analyze the ITCZ. Helpful future research would focus on closing the budget of moist static energy in models, reanalyses, and observations in order to apply the different frameworks discussed in our study to these cases, and an analysis of interactions with the ocean through the surface.

REFERENCES

Adam, O., T. Schneider, F. Brient, and T. Bischoff, 2016: Relation of the double-ITCZ bias to the atmospheric energy budget in climate models. *Geophys. Res. Lett.*, **43**, 7670–7677, doi:10.1002/2016GL069465.

Back, L. E., and C. S. Bretherton, 2006: Geographic variability in the export of moist static energy and vertical motion profiles in the tropical Pacific. *Geophys. Res. Lett.*, **33**, L17810, doi:10.1029/2006GL026672.

Bischoff, T., and T. Schneider, 2014: Energetic constraints on the position of the intertropical convergence zone. *J. Climate*, **27**, 4937–4951, doi:10.1175/JCLI-D-13-00650.1.

——, and ——, 2016: The equatorial energy balance, ITCZ position, and double-ITCZ bifurcations. *J. Climate*, **29**, 2997–3013, doi:10.1175/JCLI-D-15-0328.1.

Bollasina, M. A., and Y. Ming, 2013: The general circulation model precipitation bias over the southwestern equatorial Indian Ocean and its implications for simulating the South Asian monsoon. *Climate Dyn.*, **40**, 823–838, doi:10.1007/s00382-012-1347-7.

Bretherton, C. S., J. R. McCaa, and H. Grenier, 2004: A new parameterization for shallow cumulus convection and its application to marine subtropical cloud-topped boundary layers. Part I: Description and 1D results. *Mon. Wea. Rev.*, **132**, 864–882, doi:10.1175/1520-0493(2004)132<0864:ANPFSC>2.0.CO;2.

Broccoli, A. J., K. A. Dahl, and R. J. Stouffer, 2006: Response of the ITCZ to Northern Hemisphere cooling. *Geophys. Res. Lett.*, **33**, L01702, doi:10.1029/2005GL024546.

Byrne, M. P., and T. Schneider, 2016a: Energetic constraints on the width of the intertropical convergence zone. *J. Climate*, **29**, 4709–4721, doi:10.1175/JCLI-D-15-0767.1.

——, and ——, 2016b: Narrowing of the ITCZ in a warming climate: Physical mechanisms. *Geophys. Res. Lett.*, **43**, 11 350–11 357, doi:10.1002/2016GL070396.

Crueger, T., and B. Stevens, 2015: The effect of atmospheric radiative heating by clouds on the Madden–Julian oscillation. *J. Adv. Model. Earth Syst.*, **7**, 854–864, doi:10.1002/2015MS000434.

Dahms, E., H. Borth, F. Lunkeit, and K. Fraedrich, 2011: ITCZ splitting and the influence of large-scale eddy fields on the tropical mean state. *J. Meteor. Soc. Japan*, **89**, 399–411, doi:10.2151/jmsj.2011-501.

Donner, L. J., and Coauthors, 2011: The dynamical core, physical parameterizations, and basic simulation characteristics of the atmospheric component AM3 of the GFDL global coupled model CM3. *J. Climate*, **24**, 3484–3519, doi:10.1175/2011JCLI3955.1.

Donohoe, A., J. Marshall, D. Ferreira, and D. McGee, 2013: The relationship between ITCZ location and cross-equatorial atmospheric heat transport: From the seasonal cycle to the Last Glacial Maximum. *J. Climate*, **26**, 3597–3618, doi:10.1175/JCLI-D-12-00467.1.

Emanuel, K. A., D. J. Neelin, and C. S. Bretherton, 1994: On large-scale circulations in convecting atmospheres. *Quart. J. Roy. Meteor. Soc.*, **120**, 1111–1143, doi:10.1002/qj.49712051902.

Faulk, S., J. Mitchell, and S. Bordoni, 2017: Effects of rotation rate and seasonal forcing on the ITCZ extent in planetary atmospheres. *J. Atmos. Sci.*, **74**, 665–678, doi:10.1175/JAS-D-16-0014.1.

Fläschner, D., 2016: Intermodel spread in global and tropical precipitation changes. Ph.D. thesis, Max-Planck-Institute for Meteorology, 98 pp.

Harrop, B. E., and D. L. Hartmann, 2016: The role of cloud radiative heating in determining the location of the ITCZ in aquaplanet simulations. *J. Climate*, **29**, 2741–2763, doi:10.1175/JCLI-D-15-0521.1.

Hwang, Y.-T., and D. M. W. Frierson, 2013: Link between the double-Intertropical Convergence Zone problem and cloud biases over the Southern Ocean. *Proc. Natl. Acad. Sci. USA*, **110**, 4935–4940, doi:10.1073/pnas.1213302110.

Kang, S. M., I. M. Held, D. M. W. Frierson, and M. Zhao, 2008: The response of the ITCZ to extratropical thermal forcing: Idealized slab-ocean experiments with a GCM. *J. Climate*, **21**, 3521–3532, doi:10.1175/2007JCLI2146.1.

——, D. M. W. Frierson, and I. M. Held, 2009: The tropical response to extratropical thermal forcing in an idealized GCM: The importance of radiative feedbacks and convective parameterization. *J. Atmos. Sci.*, **66**, 2812–2827, doi:10.1175/2009JAS2924.1.

Landu, K., L. L. Ruby, S. Hagos, V. Vinoj, S. A. Rauscher, T. Ringler, and M. Taylor, 2014: The dependence of ITCZ structure on model resolution and dynamical core in aquaplanet simulations. *J. Climate*, **27**, 2375–2385, doi:10.1175/JCLI-D-13-00269.1.

Li, G., and S.-P. Xie, 2014: Tropical biases in CMIP5 multimodel ensemble: The excessive equatorial Pacific cold tongue and double ITCZ problems. *J. Climate*, **27**, 1765–1780, doi:10.1175/JCLI-D-13-00337.1.

Lin, J.-L., 2007: The double-ITCZ problem in IPCC AR4 coupled GCMs: Ocean–atmosphere feedback analysis. *J. Climate*, **20**, 4497–4525, doi:10.1175/JCLI4272.1.

Lindzen, R. S., and A. V. Hou, 1988: Hadley circulations for zonally averaged heating centered off the equator. *J. Atmos. Sci.*, **45**, 2416–2427, doi:10.1175/1520-0469(1988)045<2416: HCFZAH>2.0.CO;2.

Möbis, B., and B. Stevens, 2012: Factors controlling the position of the intertropical convergence zone on an aquaplanet. *J. Adv. Model. Earth Syst.*, **4**, M00A04, doi:10.1029/2012MS000199.

Neale, R. B., and B. J. Hoskins, 2000: A standard test for AGCMs including their physical parametrizations: I: The proposal. *Atmos. Sci. Lett.*, **1**, 101–107, doi:10.1006/asle.2000.0022.

Neelin, J. D., and I. M. Held, 1987: Modeling tropical convergence based on the moist static energy budget. *Mon. Wea. Rev.*, **115**, 3–12, doi:10.1175/1520-0493(1987)115<0003: MTCBOT>2.0.CO;2.

——, and N. Zeng, 2000: A quasi-equilibrium tropical circulation model formulation. *J. Atmos. Sci.*, **57**, 1741–1766, doi:10.1175/ 1520-0469(2000)057<1741:AQETCM>2.0.CO;2.

——, C. Chou, and H. Su, 2003: Tropical drought regions in global warming and El Niño teleconnections. *Geophys. Res. Lett.*, **30**, 2275, doi:10.1029/2003GL018625.

Numaguti, A., 1993: Dynamics and energy balance of the Hadley circulation and the tropical precipitation zones: Significance of the distribution of evaporation. *J. Atmos. Sci.*, **50**, 1874–1887, doi:10.1175/1520-0469(1993)050<1874:DAEBOT>2.0.CO;2.

Oueslati, B., and G. Bellon, 2013a: Convective entrainment and large-scale organization of tropical precipitation: Sensitivity of the CNRM-CM5 hierarchy of models. *J. Climate*, **26**, 2931–2946, doi:10.1175/JCLI-D-12-00314.1.

——, and ——, 2013b: Tropical precipitation regimes and mechanisms of regime transitions: Contrasting two aquaplanet general circulation models. *Climate Dyn.*, **40**, 2345–2358, doi:10.1007/s00382-012-1344-x.

——, and ——, 2015: The double ITCZ bias in CMIP5 models: Interaction between SST, large-scale circulation and precipitation. *Climate Dyn.*, **44**, 585–607, doi:10.1007/s00382-015-2468-6.

Popp, M., and N. J. Lutsko, 2017: Quantifying the zonal-mean structure of tropical precipitation. *Geophys. Res. Lett.*, doi:10.1002/2017GL075235, in press.

Privé, N. C., and R. A. Plumb, 2007: Monsoon dynamics with interactive forcing. Part I: Axisymmetric studies. *J. Atmos. Sci.*, **64**, 1417–1430, doi:10.1175/JAS3916.1.

Rädel, G., T. Mauritsen, B. Stevens, D. Dommenget, D. Matei, K. Bellomo, and A. Clement, 2016: Amplification of El Niño by cloud longwave coupling to atmospheric circulation. *Nat. Geosci.*, **9**, 106–110, doi:10.1038/ngeo2630.

Randall, D. A., Harshvardhan, D. A. Dazlich, and T. G. Corsetti, 1989: Interactions among radiation, convection, and large-scale dynamics in a general-circulation model. *J. Atmos. Sci.*, **46**, 1943–1970, doi:10.1175/1520-0469(1989)046<1943: IARCAL>2.0.CO;2.

Raymond, D. J., S. L. Sessions, A. H. Sobel, and Z. Fuchs, 2009: The mechanics of gross moist stability. *J. Adv. Model. Earth Syst.*, **1** (9), doi:10.3894/JAMES.2009.1.9.

Sherwood, S. C., V. Ramanathan, T. P. Barnett, M. K. Tyree, and E. Roeckner, 1994: Response of an atmospheric general circulation model to radiative forcing of tropical clouds. *J. Geophys. Res.*, **99**, 20 829–20 845, doi:10.1029/94JD01632.

Siongco, A. C., C. Hohenegger, and B. Stevens, 2015: The Atlantic ITCZ bias in CMIP5 models. *Climate Dyn.*, **45**, 1169–1180, doi:10.1007/s00382-014-2366-3.

Slingo, A., and J. M. Slingo, 1988: The response of a general circulation model to cloud longwave radiative forcing. I: Introduction and initial experiments. *Quart. J. Roy. Meteor. Soc.*, **114**, 1027–1062, doi:10.1002/qj.49711448209.

Sobel, A. H., and C. S. Bretherton, 2000: Modeling tropical precipitation in a single column. *J. Climate*, **13**, 4378–4392, doi:10.1175/1520-0442(2000)013<4378:MTPIAS>2.0.CO;2.

Stevens, B., S. Bony, and M. Webb, 2012: Clouds On–Off Klimate Intercomparison Experiment (COOKIE). Tech. Rep. 12 pp., http://www.euclipse.eu/downloads/Cookie.pdf.

Tian, B., 2015: Spread of model climate sensitivity linked to double–intertropical convergence zone bias. *Geophys. Res. Lett.*, **42**, 4133–4141, doi:10.1002/2015GL064119.

Voigt, A., S. Bony, J.-L. Dufresne, and B. Stevens, 2014a: The radiative impact of clouds on the shift of the intertropical convergence zone. *Geophys. Res. Lett.*, **41**, 4308–4315, doi:10.1002/2014GL060354.

——, B. Stevens, J. Bader, and T. Mauritsen, 2014b: Compensation of hemispheric albedo asymmetries by shifts of the ITCZ and tropical clouds. *J. Climate*, **27**, 1029–1045, doi:10.1175/ JCLI-D-13-00205.1.

Webb, M. J., and Coauthors, 2017: The Cloud Feedback Model Intercomparison Project (CFMIP) contribution to CMIP6. *Geosci. Model Dev.*, **10**, 359–384, doi:10.5194/gmd-2016-70.

Williamson, D., 2012: The APE Atlas. NCAR Tech. Note NCAR/ TN-484+STR, 508 pp., doi:10.5065/D6FF3QBR.

Zhang, R., S. M. Kang, and I. M. Held, 2010: Sensitivity of climate change induced by the weakening of the Atlantic meridional overturning circulation to cloud feedback. *J. Climate*, **23**, 378–389, doi:10.1175/2009JCLI3118.1.

Zhang, X., H. Liu, and M. Zhang, 2015: Double ITCZ in coupled ocean–atmosphere models: From CMIP3 to CMIP5. *Geophys. Res. Lett.*, **42**, 8651–8659, doi:10.1002/2015GL065973.

Zhao, M., and Coauthors, 2016: Uncertainty in model climate sensitivity traced to representations of cumulus precipitation microphysics. *J. Climate*, **29**, 543–560, doi:10.1175/ JCLI-D-15-0191.1.